60 Mbps Time-Domain Video Transfer using Body Communication

Gourab Barik, Samyadip Sarkar, Shreyas Sen
School of Electrical and Computer Engineering, Purdue University, USA
{gbarik, sarkar46, shreyas}@purdue.edu

***Abstract*— With the rapid advancement of the Internet of Bodies (IoB), a growing number of connected devices, such as health monitoring systems, smart glasses, and video sensor nodes, are being utilized around the human body. These devices typically require communication with a central high-power computing hub or among themselves. Conventional communication technologies like Bluetooth and WiFi, while widely adopted, suffer from high power consumption (∼10 mW-100 mW) and suboptimal energy efficiency (∼10-100 nJ/bit) for wearable systems. Recently, Electroquasistatic (EQS) Human Body Communication (HBC) has emerged as a promising alternative, offering both energy-efficient (∼10-100 pJ/bit) and physically secure communication modalities. In the EQS regime, voltage-mode communication, typically employing On-Off Keying (OOK), is the most commonly used approach. However, higher-order modulation schemes in this mode increase transmitter switching power, which is still lower than Bluetooth and WiFi but demands higher receiver sensitivity. Alternatively, due to the wideband characteristics of the human body, the time information of transmitted signals can be effectively preserved. This paper explores time-domain communication through the human body, demonstrating the feasibility of achieving a 60 Mbps communication channel in a machine-to-machine TD-BC scenario. Additionally, we present the successful transmission of video data through the human body with a framewise SSIM of 0.9791 framewise, underscoring the potential of this approach for future IoB applications.**

***Keywords*— Time Domain Body Communication (TD-BC), Human Body Communication (HBC), Video Communication, Electro-Quasistatic (EQS), Internet-of-Body (IoB), Time-Domain Eye Diagram.**

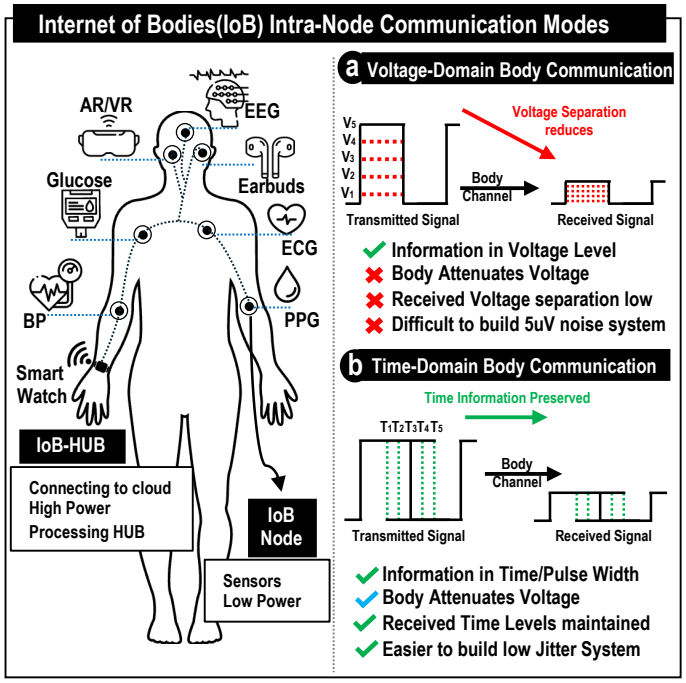

Fig. 1. Internet of Bodies (IoB) showing the various devices present around the body. Intra-Node Communication Modes (a) Voltage Domain Body Communications (b) Time-Domain Body Communication.

I. Introduction

With the rise in IoB and wearable devices around the body, such as smart watches, ECG sensors, EEG sensors, Blood Pressure (BP), and Glucose monitors, it is of the utmost importance to have an efficient communication technique between the resource-constrained IoB nodes (various sensors) and HUBs (smartwatch) as shown in Fig. 1. Recently, human-body communication has been rising in prominence as one of the most efficient and physically secure modes of communication around the body compared to Bluetooth and WiFi [1]. In [2], [3], Electroquasistatic (EQS)-HBC has been explored as a voltage-mode communication modality. From the channel responses in [4], [5], in voltage mode communication, the information is encoded in the voltage domain, and the human body attenuates the voltage level transmitted. As shown in Fig. 1(a), this results in lower spacing between the voltage levels received. Hence, by considering a transmit voltage of 1 V and a channel loss of $\sim$ 60 dB, the received voltage is 1 mV, and considering an 8-bit communication, the minimum resolution is $\sim$ 5 μV. Such low-noise systems are difficult to build and consume high power. However, in this paper, we explore the time domain for the communication of information, where the information is encoded in the pulse width. Since the human body does not affect the time information from the transmitter to the received signal owing to its wideband nature, the information received can be decoded using a very low-jitter system. In [6], [7], a low jitter system to decode the information is lower power compared to a low voltage noise system at the desired frequency of operation.

II. Time-Domain Body Communication

A. Human Body Channel Characteristics

In recent years, human-body communication (HBC) has drawn much attention as a promising method that facilitates energy-efficient communication [8] among various IoB nodes around the human body. Several studies have focused on exploring voltage domain-based communication solutions. In this context, Fig. 2(a) illustrates a numerical simulation setup for EQS-HBC in a wearable-to-wearable scenario, built upon previous findings [5], [9], [10]. The obtained frequency response analysis for the simplified capacitively approximated

2025 IEEE/MTT-S International Microwave Symposium - IMS 2025 | 979-8-3315-1409-9/25/$31.00 ©2025 IEEE | DOI: 10.1109/IMS40360.2025.11103885

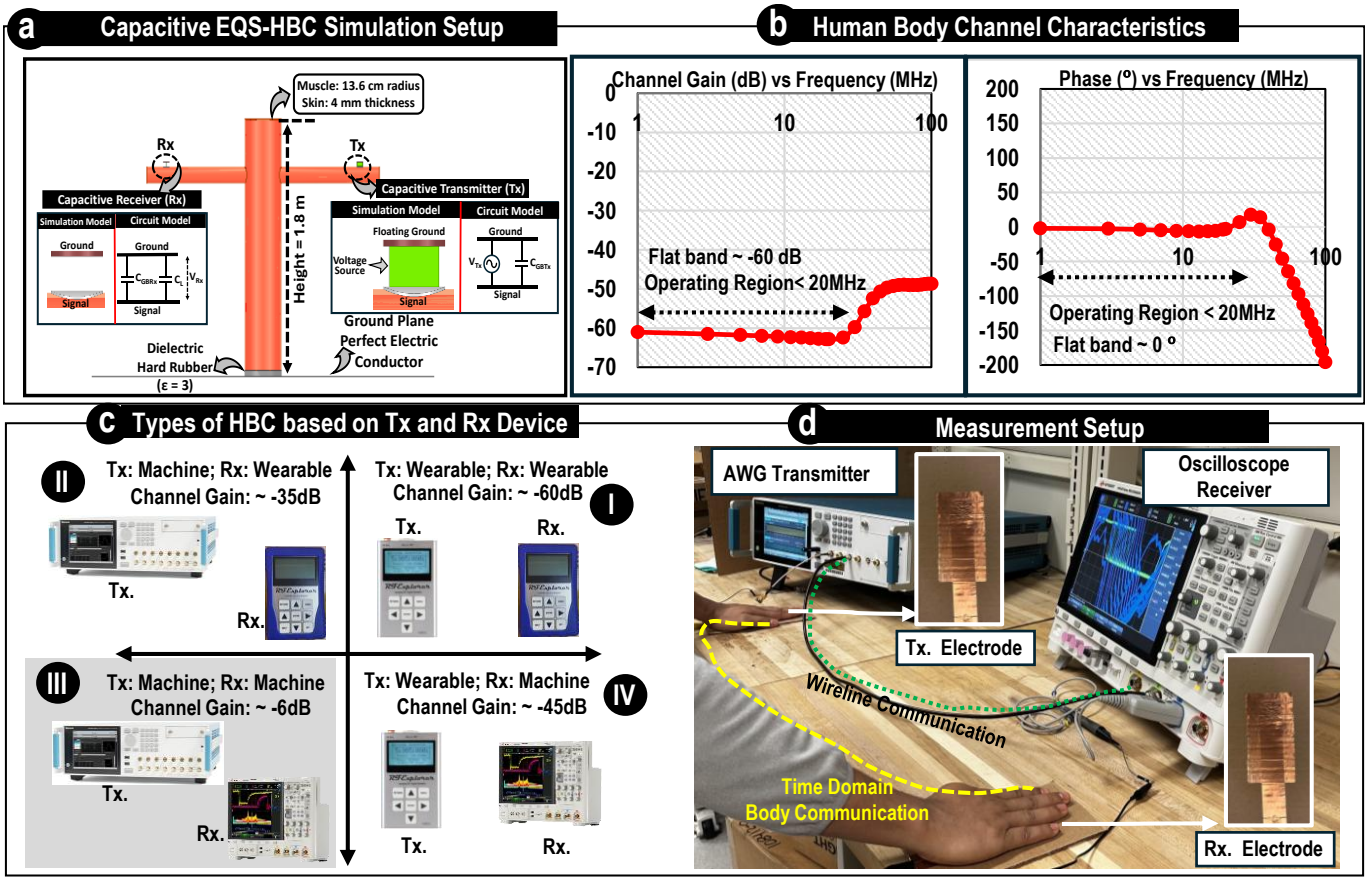

Fig. 2. (a) Capacitive EQS-HBC Simulation Setup. (b) Human Body Channel Characteristics in the desired region of operation (c) Types of HBC based on the Transmitter (Tx.) and the Receiver (Rx.) device size. (d) Measurement Setup with the Electrode (10 x 15 cm).

model, depicted in Fig. 2(b), indicates that for frequencies $\leq$ 20 MHz, the channel gain remains around -60 dB, with an approximate phase shift of $\sim$ 0 degrees. Leveraging the benefit of minimal phase distortion in EQS while preserving information in time levels motivated us to shift our focus from voltage mode communication and introduce time-domain encoding with pulse width modulation for HBC. Fig. 2(c) presents a comparison of various device sizes and their corresponding transmission losses [11]. To reinforce the potential of this approach, we successfully demonstrated machine-to-machine communication using time-domain HBC, as illustrated in Fig. 2(d) within the experimental scenario.

B. Machine to Machine Body Channel Response

An overview of the various capacitive HBC scenarios based on the devices used for transmission and reception is detailed in Fig. 2(c). Here, "machine" describes devices with strong ground coupling, whereas "wearable" refers to devices that have weaker ground coupling and parasitic capacitances from their floating grounds to the earth's ground (return-path capacitances), which become decisive in deciding channel loss [9],[11]. Scenario I depicts a context where the transmitter and receiver are wearable devices, resulting in a channel gain of approximately -60 dB. Scenarios II and IV show a channel gain of -35 dB and -45 dB, respectively, which is higher than scenario I because of the increased ground coupling of either the transmitter or the receiver. In contrast, scenario III illustrates a machine-to-machine scenario, where the channel gain is significantly higher at around -6 dB due to the enhanced ground coupling of the communicating devices and has been used for our demonstration of video communication and the characterization of the human body for time-domain communication.

C. Measurement Setup for Time domain Communication

Fig. 2(d) shows the measurement setup. It demonstrates machine-to-machine communication where the ground-connected arbitrary waveform generator (AWG) (Tektronix 5204) acts as the transmitter (generating the video signal or the pulse signals), and the ground-connected oscilloscope acts as the receiver. For measurement, the time-domain signal is coupled capacitively to the human body using a 10 cm x 15 cm copper electrode. After transmission through the human body, the signal is coupled to the receiver using a receiver electrode of a similar dimension, as the highlighted yellow path shows in Fig. 2(d). The experimental guidelines involving human subjects, approved by the Institutional Review Board (IRB Protocol 1610018370), have been followed while performing the measurements and after obtaining informed consent from all participants.

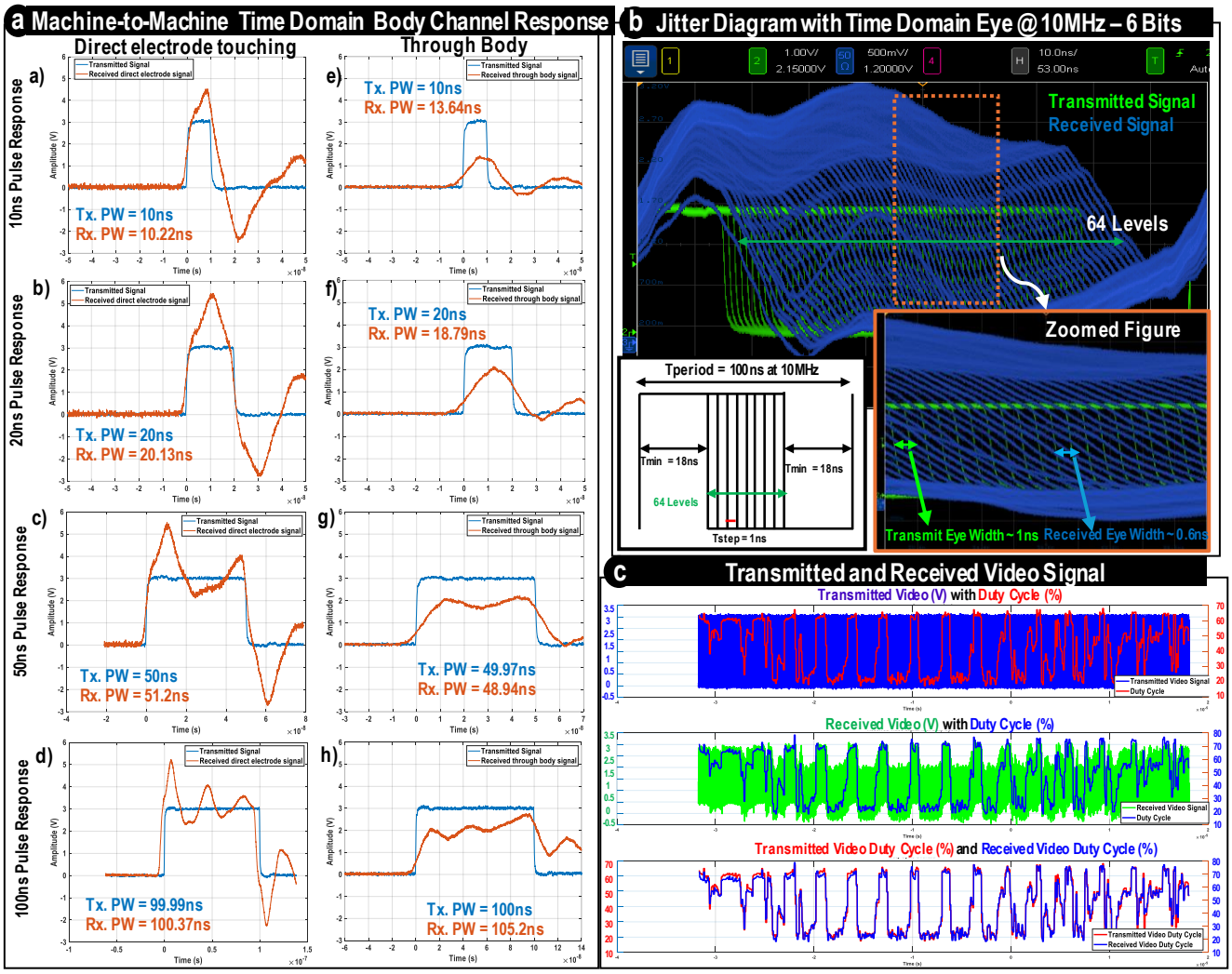

Fig. 3. Measurement Results: (a) Machine-to-Machine Time Domain Body Channel Pulse Response by Direct electrode touching and through the Human Body (b) Time Domain Eye Diagram at 10 MHz with 6-bit precision (c) Transmitted and Received PWM signal visualization using the duty-cycle of the waveforms.

III. Time Domain Body Channel Capacity

A. Pulse Response for Time-Domain Body Communication

To characterize the human body channel, the pulse response (10 ns, 20 ns, 50 ns, 100 ns) of the channel is observed. Two types of response are observed: 1) with a direct connection between the transmitter and receiver electrode, Fig. 3(a)-(d) and 2) the response through the body channel, Fig. 3(e)-(h). In the direct electrode touching scenario, the pulse width is maintained for all the test pulse widths, but it is observed that the voltage levels are higher than the transmitted signal, mostly because there is no matching present in the transmitter and the receiver side, resulting in reflections. While communicating through the body, the pulse width is observed to be preserved following the transmitted signal pulse width, with some variation. However, the effect of no-matching can be seen on the received waveform, along with the dispersion in the time domain with an attenuation of $\sim$ 6 dB in the amplitude, as expected in the machine-to-machine scenario. Extracting the correct pulse width requires appropriate thresholding to detect the first falling edge, as shown for the pulse response of 100 ns pulse width, where setting a threshold of 1.5 V helps detect the correct received pulse width.

B. Eye Diagram for Time-Domain Body Communication

Another test was performed to observe the time-domain eye diagram of the channel by applying a duty cycle/pulse width varying waveform to the body channel and observing the jitter in the received waveform. The frequency of operation is selected to be 10 MHz, based on the EQS region of operation of the HBC. A pulse width varying waveform is applied such that a minimum pulse width Tmin of 18 ns is kept on either end of the period as shown in Fig. 3(b) to maintain a maximum fundamental frequency of $\leq$ 50 MHz, and a minimum time step of 1 ns is applied to avoid aliasing at the receiver by the timing jitter introduced by the human body. Hence, from 18 ns to 82 ns, with steps of 1 ns of time resolution, a 64-level or 6-bit data can be encoded. The measurement shows that the received waveform in (blue) has a minimum eye width of $\sim$600 ps between each of the 64 levels when observed in the

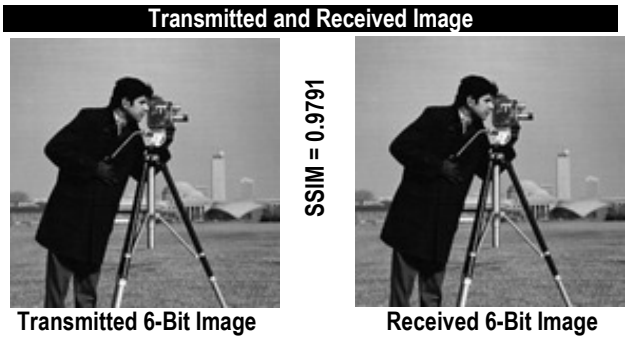

Fig. 4. Transmitted and Received Image extracted from the duty cycle with the measured SSIM.

persistence mode. By appropriate thresholding, to determine the first falling edge while extracting the pulse width, each of the 64 levels/pulse widths (6-bit) can be distinguished. Hence, we observe an overall communication channel capacity of 60 Mbps using the time-domain body communication.

C. Video Transmission through TD-BC

For the video transmission test, an 8-bit image having pixel values (0-255) is mapped to a 6-bit image having pixel values (0-63). Then, the pixel values are serialized column-wise and mapped to pulse width at 10 MHz, where a pixel value of '0' corresponds to 18 ns and the pixel value of '63' maps to a pulse width of 82 ns, in steps of 1 ns. To observe the video signal visually in the time-domain, the duty cycle is calculated per cycle. Fig. 3(c) top shows the transmitted time-domain video signal and the duty cycle corresponding to the pixel value. Fig. 3(c) center shows the received time-domain video signal through the body and its duty cycle plot. Finally, Fig. 3(c) bottom shows the duty cycle of the time-domain transmitted video signal and the received video signal duty cycle, which shows very close relations between those two. To characterize the similarity between the two time-domain video signals, an SSIM [12] of 0.9791 was measured for a single transmitted and received image frame as shown in Fig. 4, which validates the successful transfer of video through the body using time-domain communication.

IV. Conclusion

The paper explores the time domain body communication modality (TD-BC) for the first time in literature. To characterize the channel, various pulse responses are measured, showing the time-preserving capability of the human body in the EQS regime and highlighting the need for matching at the transmitter and receiver. We also highlight the need for optimal thresholding to extract the correct pulse width at the receiver for better SSIM results. We measure the time domain eye diagram, demonstrating a 60 Mbps communication channel through the human body using Time Domain Body Communication, taking advantage of the wideband nature of the human body communication channel. Finally, we demonstrate video transmission through the human body using time-domain body communication.

Acknowledgement

This work was supported by Quasistatics, Inc. under Grant 40003567.

References

[1] K. Nair, J. Kulkarni, M. Warde, Z. Dave, V. Rawalgaonkar, G. Gore, and J. Joshi, "Optimizing power consumption in IoT based wireless sensor networks using Bluetooth Low Energy," in *2015 International Conference on Green Computing and Internet of Things (ICGCIoT)*, 2015, pp. 589–593.

[2] D. Das, S. Maity, B. Chatterjee, and S. Sen, "Enabling covert body area network using electro-quasistatic human body communication," *Scientific reports*, vol. 9, no. 1, pp. 1–14, 2019.

[3] S. Maity *et al.*, "BodyWire: A 6.3-pJ/b 30-Mb/s -30-dB SIR-Tolerant Broadband Interference-Robust Human Body Communication Transceiver Using Time Domain Interference Rejection," *IEEE Journal of Solid-State Circuits*, vol. 54, no. 10, pp. 2892–2906, Oct 2019.

[4] S. Avlani, M. Nath, S. Maity, and S. Sen, "A 100KHz-1GHz termination-dependent human body communication channel measurement using miniaturized wearable devices," in *2020 Design, Automation & Test in Europe Conference & Exhibition (DATE)*. IEEE, 2020, pp. 650–653.

[5] S. Maity, M. He, M. Nath, D. Das, B. Chatterjee, and S. Sen, "Bio-physical modeling, characterization, and optimization of electro-quasistatic human body communication," *IEEE Transactions on Biomedical Engineering*, vol. 66, no. 6, pp. 1791–1802, 2018.

[6] H.-Y. Chang, C.-C. Chan, I. Y.-E. Shen, Y.-L. Yeh, and S.-Y. Huang, "Design and Analysis of CMOS Low-Phase-Noise Low-Jitter Subharmonically Injection-Locked VCO With FLL Self-Alignment Technique," *IEEE Transactions on Microwave Theory and Techniques*, vol. 64, no. 12, pp. 4632–4645, 2016.

[7] W. Bae, "State-of-the-Art Circuit Techniques for Low-Jitter Phase-Locked Loops: Advanced Performance Benchmark FOM Based on an Extensive Survey," in *2021 IEEE International Symposium on Circuits and Systems (ISCAS)*, 2021, pp. 1–5.

[8] G. Barik, B. Chatterjee, G. K. K, and S. Sen, "A 65nm 21.9pJ/Sa Pixel to PWM Conversion SoC with Time-domain Body Communication for ULP Body-Worn Video Sensor Nodes with Distributed Real-Time Inference," in *2024 IEEE Custom Integrated Circuits Conference (CICC)*, 2024, pp. 1–2.

[9] M. Nath, S. Maity, and S. Sen, "Toward understanding the return path capacitance in capacitive human body communication," *IEEE Transactions on Circuits and Systems II: Express Briefs*, vol. 67, no. 10, pp. 1879–1883, 2019.

[10] A. Datta, M. Nath, D. Yang, and S. Sen, "Advanced biophysical model to capture channel variability for EQS capacitive HBC," *IEEE Transactions on Biomedical Engineering*, 2021.

[11] S. Maity, D. Das, B. Chatterjee, and S. Sen, "Characterization and classification of human body channel as a function of excitation and termination modalities," in *2018 40th Annual International Conference of the IEEE Engineering in Medicine and Biology Society (EMBC)*. IEEE, 2018, pp. 3754–3757.

[12] A. C. Brooks, X. Zhao, and T. N. Pappas, "Structural similarity quality metrics in a coding context: Exploring the space of realistic distortions," *IEEE Transactions on Image Processing*, vol. 17, no. 8, pp. 1261–1273, 2008.